Retrieving forest soil moisture from SMAP observations considering a microwave polarization difference index (MPDI) to τ-ω model

Chang-Hwan Park, Thomas Jagdhuber, Andreas Colliander, Aaron Berg, Michael H. Cosh, Johan Lee, Kyung-On Boo

PII: S2666-0172(24)00015-4

DOI: https://doi.org/10.1016/j.srs.2024.100131

Reference: SRS 100131

To appear in: *Science of Remote Sensing*

Received Date: 31 December 2023

Revised Date: 19 March 2024

Accepted Date: 7 April 2024

Please cite this article as: Park, C.-H., Jagdhuber, T., Colliander, A., Berg, A., Cosh, M.H., Lee, J., Boo, K.-O., Retrieving forest soil moisture from SMAP observations considering a microwave polarization difference index (MPDI) to τ-ω model, *Science of Remote Sensing*, https://doi.org/10.1016/j.srs.2024.100131.

Retrieving forest soil moisture from SMAP observations considering a microwave polarization difference index (MPDI) to τ-ω model

Chang-Hwan Park [1,2*], Thomas Jagdhuber [3,4], Andreas Colliander [5], Aaron Berg [6], Michael H. Cosh [7], Johan Lee [8] and Kyung-On Boo [8]

[1] Department of Civil Systems Engineering, Ajou University, Suwon, Korea

[2] Department of Civil Systems Engineering, Ajou University, Tashkent, Uzbekistan

[3] German Aerospace Center (DLR), Microwaves and Radar Institute, Oberpfaffenhofen, 82234 Wesling, Germany

[4] University of Augsburg, Institute of Geography, 86159 Augsburg, Germany

[5] Jet Propulsion Laboratory, California Institute of Technology, Pasadena, CA 91109, USA

[6] Department of Geography, Environment and Geomatics, University of Guelph, Guelph, ON N1G 2W1, Canada

[7] United States Department of Agriculture, Agricultural Research Service, Hydrology and Remote Sensing Laboratory, Beltsville, MD 20705, USA

[8] Operational System Development Department, National Institute of Meteorological Sciences, Jeju 63568, Korea

Abstract

Estimating soil moisture from microwave brightness temperature is extremely challenging in densely vegetated areas. The soil moisture retrieved from the Soil Moisture Active Passive (SMAP) measurements tends to be consistently overestimated, sometimes exceeding the saturation level of mineral soils. Therefore, the retrieved soil moisture cannot detect or monitor

climate extremes, such as floods and droughts for forests, natural resource management, and climate change research. We hypothesize that the main issue is that the scattering albedo (ω) and the optical depth (τ) are parameterized solely with NDVI (Normalized Difference Vegetation Index), neglecting the polarization characteristics from vegetation structure. This study proposes a weighting factor between scattering and optical thickness, a function of MPDI (Microwave Polarization Difference Index), and applies it to both parameters simultaneously to increase the scattering effect and decrease the attenuation effect in high MPDI. The validation results based on the Climate Reference Network revealed that considering MPDI is critical in reducing soil moisture overestimation errors and obtaining more accurate soil moisture over forested regions. This results in correlation improving from 0.36 to 0.44, a decrease in ubRMSE from 0.179 to 0.125 cm^3cm^{-3}, and bias lowering from 0.127 to 0.060 cm^3cm^{-3} in comparison with the SMAP measurements over forested regions.

1. Introduction

Global-scale soil moisture (SM) information can be obtained from satellite measurements such as microwave brightness temperature of SMOS (Soil Moisture and Ocean Salinity), AMSR-2 (Advanced Microwave Scanning Radiometer 2) and SMAP (Soil Moisture Active Passive). Among them, SMAP provides SM products using the Single Channel Algorithm (SCA) (Jackson, 1993) and Dual Channel Algorithm (DCA) (P. O'Neill et al., 2020; Chaubell et al., 2020). The Multi-Temporal Dual Channel Algorithm (MT-DCA) for estimating albedo as a spatially variable parameter has also been proposed (Konings et al., 2017). Still, some uncertainties in the microwave radiation transfer model (RTM or forward model) must be solved to more accurately estimate SM from satellites. It is known that even L-band, the most penetrating available waveband on current satellite platforms, cannot provide a reliable SM information in the forests or dense vegetation areas even though studies have shown that the SMAP SM product, for example, does demonstrate sensitivity to SM changes in forests (Colliander et al., 2020; Ayres et al., 2021; Ambadan et al., 2022; Abdelkader et al., 2022). A recent study (Al-Yaari et al., 2019) found that SM retrieval with vegetation water content (VWC) greater than 5 kg m^{-2} (approximately 0.6 VOD) is not usable and unreliable in some SM products. Fig.1b shows abnormally high SM values in dense vegetation areas as shown in Fig 1a.

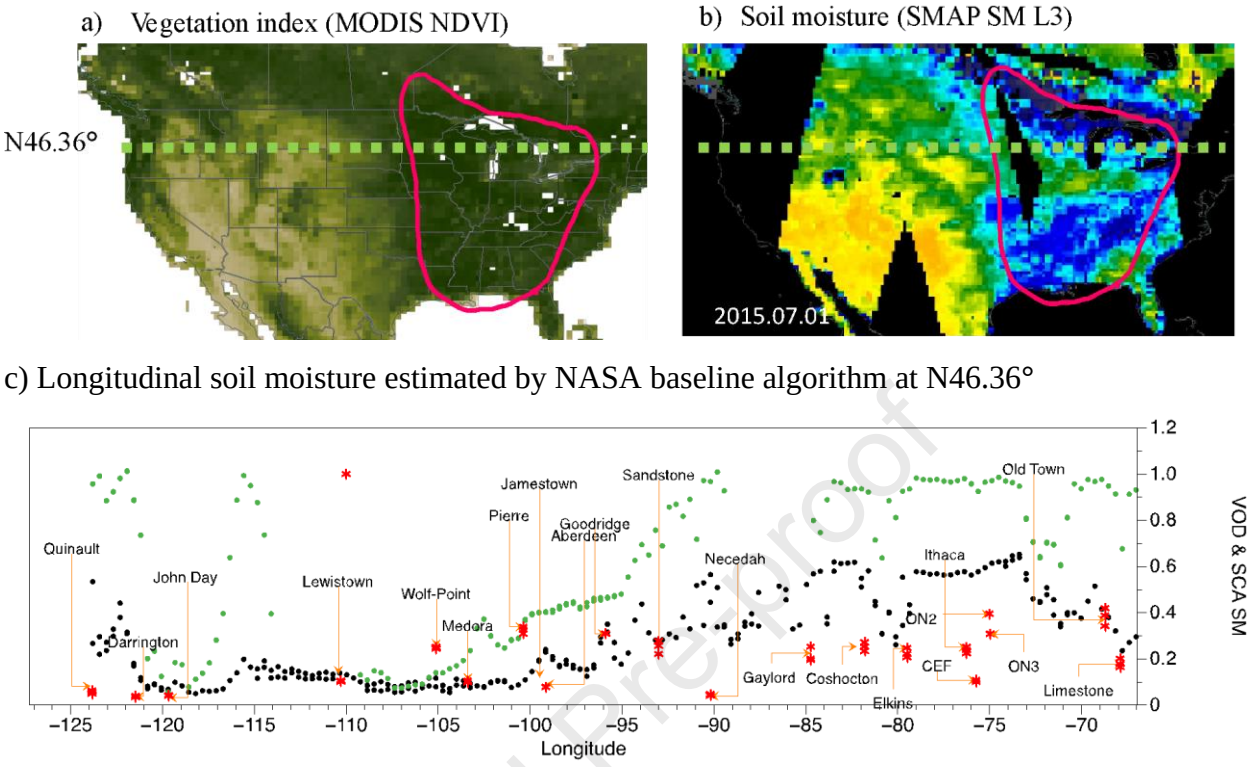

Fig.1 a) MODIS NDVI and c) the cross section overestimated SMAP SCA soil moisture (black dots) comparing to in situ (red dots) over vegetation with VOD_{NDVI} (green dots) indicated with the red boundary in a), b) and longitudinal range from -90 to -65, where vegetation optical depth over 0.5 in b), measured in 1st, August 2015.

Recent research suggests that the poor performance of satellite SM products over dense vegetation is due to the unsolved uncertainty regarding vegetation properties within RTM, rather than an inherent limitation of the technique. For example, Ambadan et al. (2022) and Colliander et al. (2020) suggested that SM can be estimated using SMAP brightness temperature (Tb) under temperate forests if vegetation properties such as attenuation and scattering parameters are properly estimated within the microwave forward model.

Currently, in both SCA and DCA, the vegetation scattering albedo is fixed regardless of vegetation density. We selected SCA-based algorithms to work on the improvement for VOD characterization, We bring the argument forward that disentangling vegetation and soil emission contribution is not strait forward when using both polarizations,TBv and TBh, since both observations are not fully statistically independent, especially in dense (forested) vegetation. In

this realm, we revisited the single-polarization SCA approaches, where VOD is not retrieved, but an input to the retrieval. In this study, we develop several advanced strategies how to represent VOD more realisticly and efficiently. To address this issue, Park et al., (2020) described a τ-ω type RTM based on a variational scattering albedo approach, where increasing vegetation optical depth (VOD) computed by NDVI increases the scattering albedo. This analysis focused on resolving the impact of unrealistic scattering albedo in forested regions with high vegetation optical depth on SM. Chaparro et al. (2022) showed that the retrievability of SM from vertically and horizontally polarized Tb can be determined with a metric called the robustness of vegetation optical depth, indicating higher robustness over non-woody vegetation rather than in forests. In our study, we found that the current SMAP SCA exhibits error patterns related to VOD calculated using NDVI as well as the Microwave Polarization Difference Index (MPDI) calculated using Eq (1) (Becker and Choudhury 1988), as seen in Fig 2.

$$MPDI = \frac{(Tb_V - Tb_H)}{(Tb_V + Tb_H)} \tag{1}$$

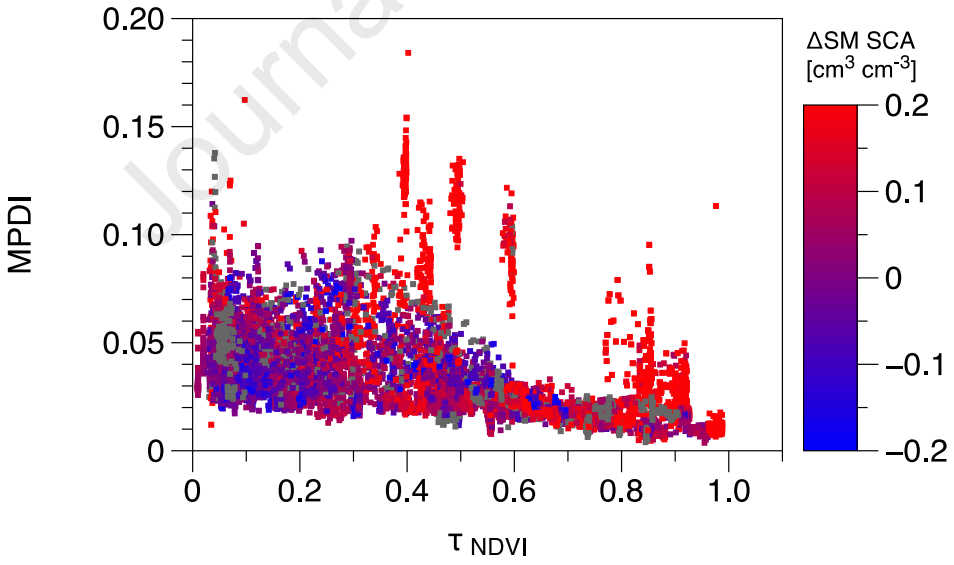

Fig. 2 The relationship between τ from MODIS NDVI and MPDI from SMAP Tb_H and Tb_V and the degree of the soil moisture bias from SMAP SCA SM compared to the *in-situ* soil moisture obtained from USCRN sites (ΔSM SCA) along the NDVI-MPDI relationship (gray: missing calculation in the SM estimations)

In Figure 2, the blue and red dots indicate that SM predictions are underestimated and overestimated respectively. This figure shows that the SCA method overestimates SM when VOD (computed from NDVI) and MPDI are high. This is because the conventional RTM does not consider the polarization characteristics of vegetation in dense vegetation areas. To elaborate, at a τ value of 0.6, less SM bias was observed in the lower MPDI range. According to Equation (1), in scenarios of low MPDI, the difference between vertical and horizontal scattering, as well as their resulting Tb, should be minimal. This implies that a lower MPDI is expected to yield a relatively smaller SM bias in SMAP SCA predictions, even when assuming a uniform scattering albedo within the SCA model. Conversely, in the case of a higher MPDI, it will reveal an issue due to the constant scattering assumption in SCA. For instance, when neglecting these factors in the SCA model—when there is a substantial difference in scattering albedo between horizontal and vertical polarizations (likely when MPDI is high)— the Tb simulations in horizontal and vertical polarization with a fixed scattering albedo lead to a bias in SM estimation (a positive SM bias for horizontally polarized Tb). Consequently, it is crucial to adjust vegetation-related parameters, such as VOD and scattering albedo, particularly at higher MPDI values. The methodology section will further elaborate on this strategy.

2. Method

We propose a τ-ω model that is parameterized with both NDVI and MPDI to resolve the issue of the missing vegetation structural information in the RTM used by SCA and DCA, we propose a τ-ω model that is parameterized with both NDVI and MPDI. To introduce this method, we will first discuss the SM errors that arise from the current RTM, particularly those that are caused by an incomplete τ-ω model.

2.1 Microwave radiative transfer model

Soil moisture is the most impactful surface property to low-frequency microwave emission due to its dipole structure. Therefore, L-band (1.4 GHz) Tb measurements are the best wavelength to extract SM information. The microwave radiative transfer model connects SM within the wet soil emissivity (e_{soil}) and microwave Tb. However, this does not mean that other variables are negligible in Eq. (2), which is a function of e_{soil}, surface temperature (T), vegetation optical depth ($\boldsymbol{\tau}$), and vegetation scattering albedo (ω).

$$\mathrm{Tb_H} = e_{\mathrm{soil}}(SM)e^{-\tau} + (1-\omega)(1-e^{-\tau})T + e^{-\tau}\left(1 - e_{\mathrm{soil}}(SM)\right)(1-\omega)(1-e^{-\tau})T \quad (2)$$

An accurate dielectric mixing model (between e_{soil} and SM) and τ-ω (for vegetation effects) model are prerequisites to invert vegetation and SM components from the measured Tb or to simulate Tb closest to the observed Tb. Various studies have discussed improvements to the inversion formulation, for example, 1) dielectric mixing model considering explicitly organic matter (Bircher et al., 2016; Mironov et al., 2018, 2019; Park et al., 2019; Park et al., 2017); 2) roughness effect parameterized with SM (Fernandez-Moran et al., 2015, 2017, Parrens et al., 2016, Peng et al., 2017) ; 3) τ-ω model by considering multiple scattering properties (Kurum, 2013; Feldman et al., 2018), by specifying it in space as look-up table (Konings et al., 2016, 2017) and by parameterizing it with VOD in order to impose variability in time and space (Park et al., 2020). Because both high VOD and rich SOM regions have shown unrealistic retrieval values in the current SMAP SCA and DCA SM, an improvement is anticipated in these areas.

Wigneron et al. 2014 found that vegetation model parameters are influenced in L-band SM estimation, by factors like system configuration and crop type, including VOD, scattering albedo, and polarization properties. These discoveries help to enhance forward modeling and retrieval techniques for estimating SM over regions covered by vegetation. Based on Eq. (2), to translate the measured Tb to a lower SM value, the simulated Tb ($\mathrm{Tb_{sim}}$) should be made lower by increasing the scattering albedo and/or decreasing the optical depth.. This new adjustment will be made according to the polarizability information from MPDI and in addition to the dynamic scattering albedo introduced by Park et al. (2020). Therefore, this study will apply the MPDI approach (Chaparro et al., 2022) with the variational ω model (Park et al., 2020) to improve the polarization representation in the τ-ω model.

2.2 MDPI based τ-ω model

Figure 3a shows that the conventional τ-ω model sets the scattering albedo, ω, to a constant that varies only according to IGBP land cover classification (SCA and DCA). Therefore, in high vegetation states, only τ affects Tb simulation. In the modified τ-ω approach (Figure 3b), ω can also increase with increasing NDVI. In this approach, τ and ω are related to a power function based on the allometric theory. Even so, with the relatively high τ, the SM estimation is accurate

with a low MPDI but the overestimation still occurred in high MPDI. Hence, to reduce the SM error, which tends to increase when MPDI increases, both τ and ω are supposed to be readjusted by MPDI input as shown in the Fig. 3c.

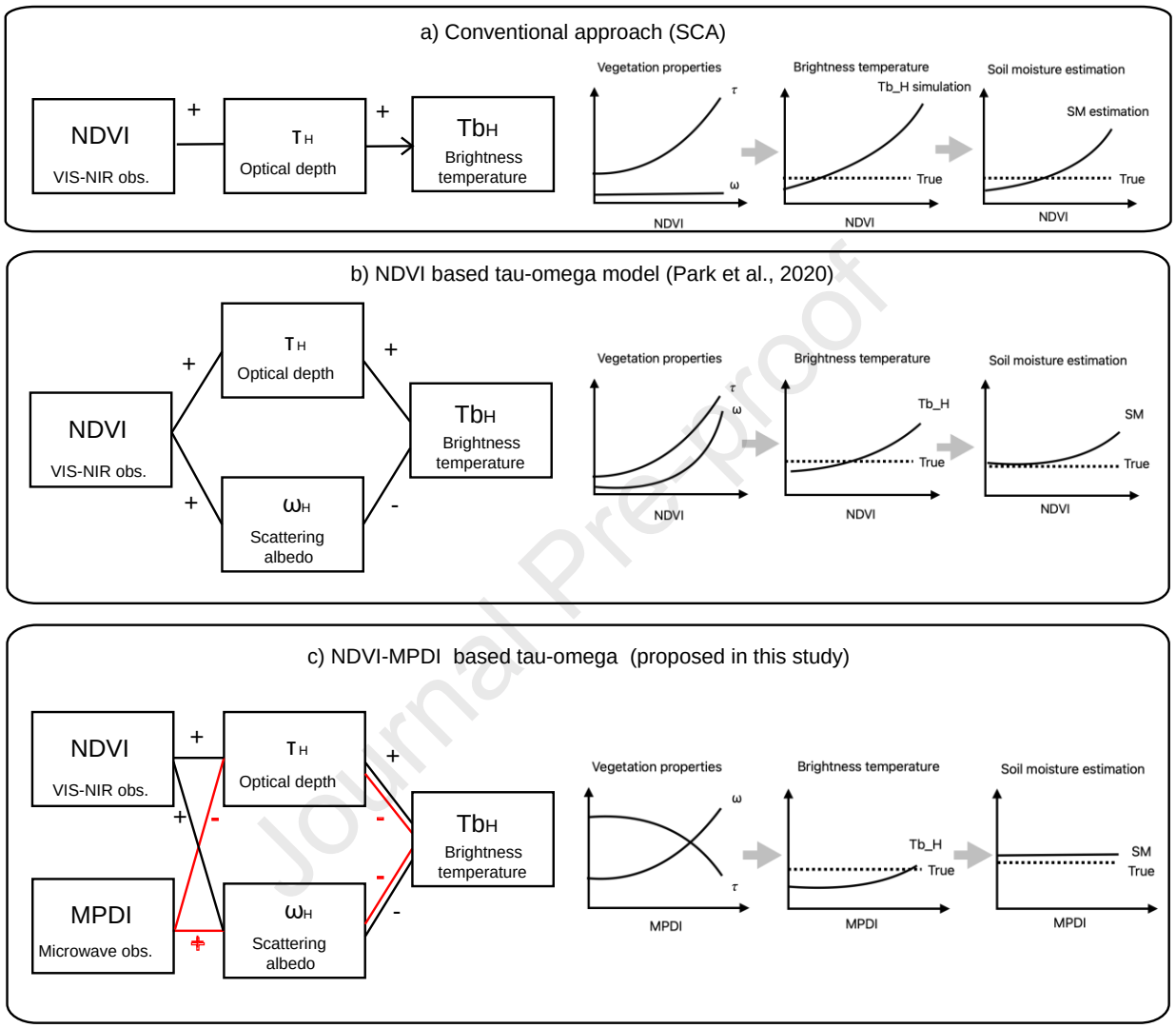

Fig. 3 Effect of high vegetation on the microwave brightness temperature simulated by (a) the conventional NDVI-based τ-ω model (SCA), (b) the allometry-based τ-ω model (Park et al., 2020), and (c) the τ-ω model adjusted by MPDI (red lines: new consideration in this study)

In this new approach (Fig. 3.c), ω is adjusted in proportion to MPDI, especially when applied to the forward simulation of horizontally polarized Tb. In our earlier method (Fig. 3.b), only NDVI is used for Tb_h simulation, linking it to vegetation density and assuming a constant ratio of vertical to horizontal components (no directionality in vegetation structure) for the same IGBP

type. This means a higher NDVI indicates denser vegetation, resulting in more attenuation (τ) and increased scattering (ω). This method reduces the error caused by the fixed ω in the dense forest by enhancing ω. However, in the scenarios where horizontal vegetation scattering is the dominant factor within the same IGBP, relying on NDVI for Tb_h simulations poses issues. The NDVI-based ω, which assumes a consistent ratio between horizontal and vertical scattering (e.g., a randomly distributed vegetation canopy), turns out to be lower than the actual ω when the horizontal vegetation component exceeds the average for the IGBP class in a particular SMAP grid cell. This case leads to an underestimated scattering albedo, causing an overestimation in Tb simulations and, consequently, an overestimation of SM.

Introducing MPDI addresses the problem with underestimated scattering albedo by being "positively proportional to horizontally polarized" scattering albedo. An abnormally high MPDI can indicate a higher horizontally polarized scattering albedo than the typically applied scattering albedo based on the IGBP classification. When the horizontally polarized scattering exceeds that of the vertically polarized components, the horizontally polarized ω becomes larger than the one assumed for both polarizations based on the IGBP type, reducing the Tb_h. This reduction in Tb_h provides a physical basis for the positive correlation between scattering and MPDI measurements:

Higher ω_H ➔ Lower Tb_H ➔ higher MPDI, $(Tb_V-Tb_H)/(Tb_V+Tb_H)$.

A solitary Tb_H value is insufficient for delineating scattering properties due to its variation with factors such as soil temperature, moisture, roughness, and both the density and structural properties of vegetation. In contrast, MPDI provides insight into scattering properties by utilizing both Tb_H and Tb_V, measured under identical conditions of temperature, moisture, and vegetation density but differ in their structural responses. By subtracting these values and normalizing them by their sum, the effects of temperature, soil moisture, roughness, and vegetation density on $Tb_{H/V}$ are mitigated to a first degree, leaving only the structural characteristics. This is where MPDI excels, as it effectively isolates and represents these structural properties. This relationship in the Tb_H forward simulation (Higher ω_H ➔ lower Tb_H with no change in Tb_V) allows the model to incorporate structural details inversely from MPDI, such as an increased horizontal component, which cannot be captured by using only the conventional approach where $\omega_H = \omega_V$. In other words, for a canopy with more horizontal components at the same density (indicating a higher MPDI in

the same VOD scenario), the horizontal ω should be set higher than the vertical ω. Therefore, it is necessary to set ω in proportion to both MPDI and NDVI, as illustrated with the '+' signs in Fig. 3. Inversely, in the high MPDI condition, the simulated Tb_H is lower (Higher MPDI → Higher ω_H → Lower Tb_H as shown along the red arrows in Fig.3), which does not deviate substantially from the measured Tb_H. Under this condition, SM is estimated in the moderate range and is not unrealistically overestimated. The NDVI-MPDI approach (EXP2) is shown in Table 1, along with the conventional NDVI-based SMAP SCA algorithm theoretical basis document (ATBD) (O'Neill et al., 2021) and the allometric-based model of Park et al. (2020) (EXP1).

Table 1. The mathematical equations for calculating τ and ω used in the microwave radiative transfer model.

	Optical thickness (τ)	Scattering albedo (ω)
SCA	$\tau = b\mathrm{VWC}$	Constant
EXP1	$\tau = b\left((1.9134NDVI^2 - 0.3215NDVI) + \mathrm{StemFactor}\frac{NDVI_{ref} - 0.1}{1 - 0.1}\right)$	$\omega = c_{IGBP}\tau^{2/3}$
EXP2	$\tau = (1 - 0.2f_{MPDI})bVWC$ $\tau = (1 - 0.2f_{MPDI})b\left((1.9134NDVI^2 - 0.3215NDVI) + \mathrm{StemFactor}\frac{NDVI_{ref}-0.1}{1-0.1}\right)$	$\omega = f_{MPDI}c_{IGBP}\tau^{2/3}$

The c_{IGBP} in Table 2 is an empirical parameter that represents different types of vegetation presented by Park et al. (2020). It is calculated by multiplying the maximum vegetation scattering albedo (ω_{max}) by the product of the vegetation canopy parameter (b), the physical density of plant elements (ρ_E), the unique thickness of the plant element (h), and a canopy environmental parameter (c) raised to the power of two-thirds as shown in Eq. (3).

$$c_{\mathrm{IGBP}} = \omega_{\max}(\mathrm{b}\ \rho_{\mathrm{E}}\ \mathrm{c}\ \mathrm{h})^{-2/3} \quad (3)$$

Table 2 shows that c_{IGBP} values found for forests tend to be lower than for crops and grasslands, which is consistent with the empirically derived relation that c_{IGBP} is inversely proportional to the height of vegetation, h, in Eq.(4).

Table 2. Empirical allometry parameter c_{IGBP} for each IGBP type (modified from Park et al., 2020) (shaded cells : the classified by forested regions (IGBP from 1 to 5))

Evergreen needle	IGBP=1 0.40	Mixed forest	IGBP=5 0.30	Savana	0.20	Urban	0.10
Evergreen broad	IGBP=2 0.15	Closed shrubland	0.60	Grass	0.60	Mixed crop	0.6
Deciduous needle	IGBP=3 0.40	Open shrubland	0.2	Permanent wetland	0.10	Snow & ice	3
Deciduous Broadleaf	IGBP=4 0.20	Woody savanna	0.5	Crop	0.40	Spared vegetation	3

The weighting factor f_{MPDI}, Eq.(4), enables an enhancement of the scattering albedo while simultaneously reducing the optical depth, as derived from the MPDI compared to traditional τ and ω values. This model, which posits an inverse relationship between MPDI and NDVI, is supported by the measured in Figure 2 and the study from Becker et al., 1988.

$$f_{MPDI} = aMPDI^{0.5} + b \quad (4)$$

In this study, these parameters are found by empirically minimizing SM errors (a is 2 and b is 0.65). Now, in the new τ-ω model, both τ and ω are functions of NDVI, considering vegetation structural information by the weighting factor, f_{MPDI} in Eq. (4), and the allometric parameter, c_{IGBP} in Eq.(3) (simplified as constants in Table 2).

2.3 Cost function minimization

To estimate SM from the Tb_{obs}, the Tb absolute error is computed by Eq. (2) by searching for the minimum absolute difference between observed Tb_{Obs} and simulated Tb_{sim} with given state variables X (soil texture, soil temperature, roughness, soil organic matter, soil temperature, and NDVI-based VOD) and additional ancillary MPDI according to the following function:

$$\min_{X=SM} J = 0 = \sum\left(Tb_{\text{obs}} - Tb_{\text{sim}}(X, NDVI, MPDI)\right)^2 \quad (5)$$

In Eq. (3), higher MPDI induces higher f_{MPDI} (the weighting factor increases in scattering and decreases in attenuation by absorption) allowing more accurate SM retrieval, owing to the lower Tb simulation in Eq. (2). Therefore, MPDI will help to reduce overestimation of SM (Eq.(5)) by increasing the weighting factor (Eq.(3)) for scattering and decreasing the weighting factor for absorption in Eq. (2).

2.4 Validation

SM validation should occur outside rain periods (Colliander et al., 2020b) and over a range of wetness conditions. Therefore, validation points for this study were only considered if SM conditions were below saturation (i.e., assuming no flooded regions). The validation compares our retrieved SM to in situ data, where SM is larger than the saturation point, which is function of soil organic matter and clay proposed by Park et al. (2021).

3. Data

USCRN (US Climate Reference Network) is used in this study to validate the SM estimates because of its dense distribution of validation networks (Diamond et al., 2013). The results of the new τ-ω model are investigated with all in situ from these sites. Furthermore, to demonstrate how SM estimation from SMAP Tb can be improved in densely vegetated areas, a longitudinal band across a strong vegetation gradient in the US was selected, as shown in Fig. 4 a). Also, the NEON (the National Science Foundation's National Ecological Observatory Network) is used because many of the monitoring stations are located under a forest canopy (Ayres et al., 2021) b).

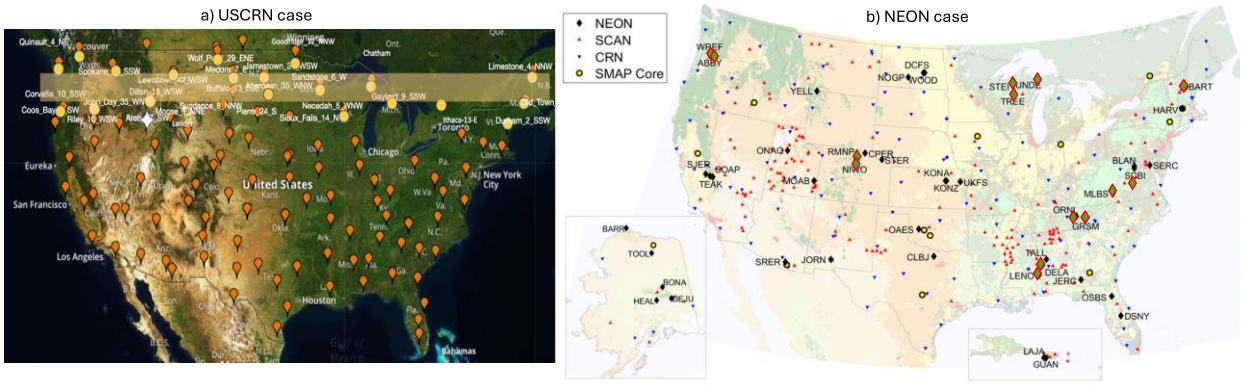

Fig.4 a) USCRN (US Climate Reference Network) with the longitudinal cross section points in the orange box (latitude: 46.36°, longitude: -125° to -65°) used in the validation of the soil moisture estimations, b) NEON (National Ecological Observatory Network) forest sites marked by green diamond symbols.

The evaluation of our methodology focused exclusively on forested areas within the United States, specifically leveraging sites from the USCRN and NEON. These forested sites present unique challenges for soil moisture estimation.

Table 3. Classification of forested regions for this study based on IGBP categories

USCRN				NEON	
Site name	IGBP		IGBP		IGBP
Asheville-13-S	5	Kingston-1-W	4	D01.BART	5
Asheville-8-SSW	5	Limestone-4-NNW	5	D01.HARV	5
Charlottesville-2-SSE	4	McClellanville-7-NE	5	D02.SCBI	4
Chatham-1-SE	5	Millbrook-3-W	5	D05.STEI	5
Coos-Bay-8-SW	1	Old-Town-2-W	5	D05.TREE	5
Corvallis-10-SSW	1	Quinault-4-NE	1	D05.UNDE	5
Darrington-21-NNE	1	Redding-12-WNW	1	D07.GRSM	5
Durham-2-SSW	5	Salem-10-W	5	D07.MLBS	4
Elkins-21-ENE	4	Sandstone-6-W	5	D07.ORNL	4
Gaylord-9-SSW	5	Selma-13-WNW	5	D08.DELA	5

John-Day-35-WNW	1	Spokane-17-SSW	1	D08.LENO	5
Kenai-29-ENE	1	Watkinsville-5-SSE	5	D10.RMNP	1
				D13.NIWO	1
				D16.ABBY	5
				D16.WREF	1

The table 3 categorizes the study locations according to the International Geosphere-Biosphere Programme (IGBP) classification system, indicating the predominant vegetation type as the forested resions. This targeted approach ensures that our soil moisture estimation technique is properly tested in forested regions where it is most challenged for the SMAP SCA.

The applied brightness temperature data is the SMAP L3 horizontally polarized brightness temperature measured in descending node time, at approximately 6 am local time (de Jeu et al., 2008; Zhang et al., 2019). The input vegetation information is the $\boldsymbol{\tau}_{\mathrm{NDVI}}$, which is the same input used for the conventional SMAP SM_{SCA} algorithm.

4. Results

The τ-ω RTM was initially analyzed to see if the proposed τ-ω could improve the accuracy of the SM estimation from SMAP Tb. Figure 5 demonstrates the advantage of using the MPDI-based τ-ω model. The baseline τ-ω RTM with a constant ω (Figure 5a) is unable to produce accurate SM estimates with the VOD derived from NDVI. As a result, SM SCA estimates over high-VOD regions (forests) using the constant ω exceed 0.55 cm^3cm^{-3}. On the other hand, Figure 5b shows an increase in ω by τ, leading in turn to a decrease in simulated Tb, resulting in a more accurate SM estimate (positive bias decrease of approximately 0.5 cm^3cm^{-3}). The most accurate result is obtained with the proposed approach, in which both τ and ω are further adjusted by MPDI (Figure 5c). Our findings indicate that this technique is successful when the Tb_V-value is lower than 230 K and the VOD is larger than 0.1, provided that the coefficient 'a' is set to 15000 and 'b' is 3 in Equation (3).

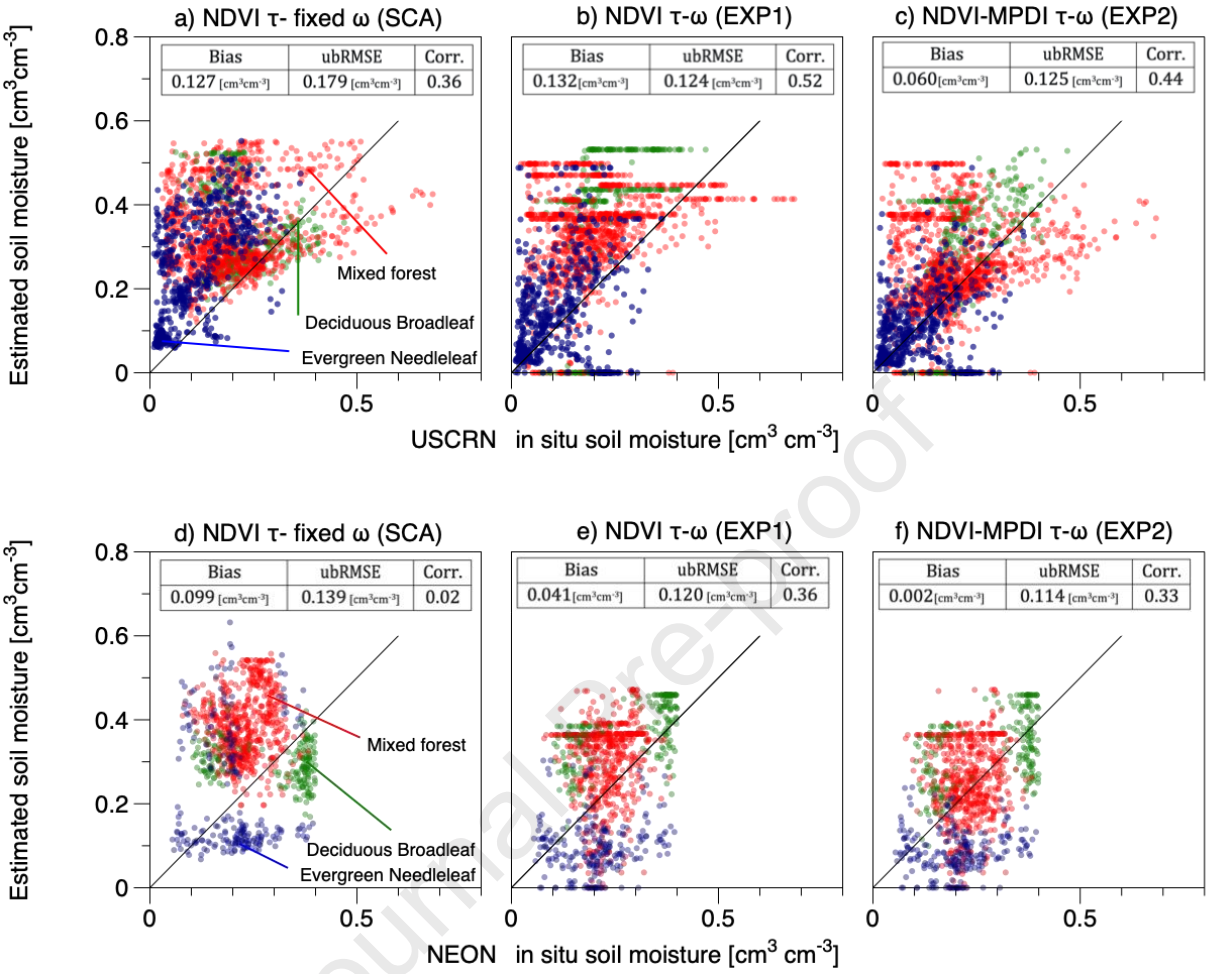

Fig. 5 Scatter plots comparing a) SCA-H, b) NDVI-based τ and ω model (EXP1), and c) NDVI-MPDI-based τ and ω model (EXP2) with in situ soil moisture measurements in USCRN forest and d), e) and f) in NEON forest sties classified with IGBP from 1 (blue), 4 (green) and 5 (red).

As Fig. 5 shows, the NDVI-MPDI-based τ and ω model demonstrated enhanced soil moisture estimation in validation with in situ measurements, achieving approximately reduction 55% in bias, a 21% reduction in ubRMSE and a 32% increase in correlation compared to SCA-H SM.

~~As shown in figure 8. increased ω by high NDVI decrease the SM estimation (EXP1) comparing to the constant ω (control) both in a) USCRN and b) NEON forest sites where IGBP is ranged from 1 to 5 (forest regions). Addtionaly, the further increased ω by high MPDI in forest from c)~~

~~USCRN and d) NEON forest sties decrease SM from EXP1 to EXP2. Ultimately the gradual decrease SM by NDVI and MPDI consideration in τ-ω leads the bias degrease soilving unrealistic SM estimation from the microwave brightness temperature measured over the forest regions.~~

Figure 6 illustrates the NDVI - MPDI effects on SM estimations. For both the USCRN (a) and NEON (b) forest sites with IGBP classifications ranging from 1 to 5 (indicative of forest regions), an increase in the NDVI-adjusted parameter ω results in a decrease of SM estimation (EXP1) compared to a control scenario with constant ω. Further, an increased ω, this time modulated by high MPDI values, is observed to reduce SM from EXP1 to EXP2 in forest sites from both USCRN (c) and NEON (d).

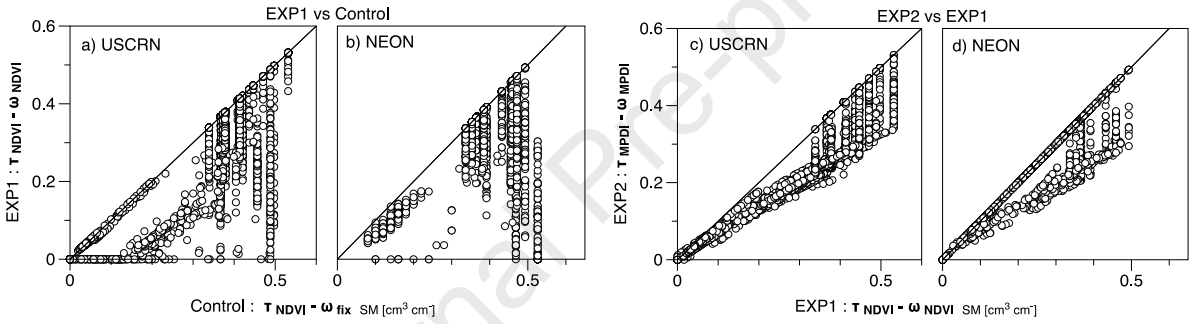

Fig. 6 The NDVI and MPDI effect on soil moisture estimation : ω NDVI effect on SM in a) USCRN and b) NEON and τ-ω NDVI and MPDI effect on SM in c) USCRN and d) NEON in forest sites (IGBP classification from 1 to 5)

This sequential reduction in SM estimations is well displayed in Fig.7. Factoring in the effects of NDVI and MPDI in the τ-ω model leads to a more accurate bias correction in SM derived from microwave brightness temperature measurements over forest regions. The figure underscores the significance of considering NDVI and MPDI influences for realistic SM estimation in dense forest regions.

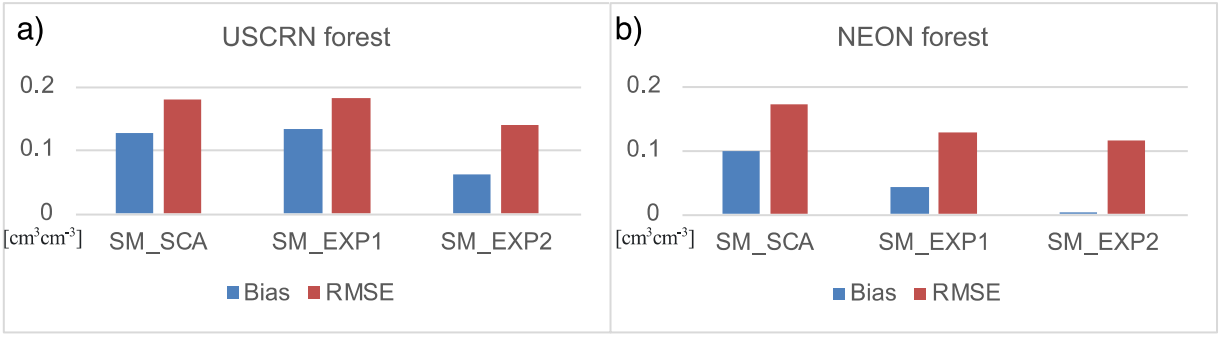

Fig. 7 Bias and RMSE change with different τ-ω models W_sca (SMAP SCA), W_NDVI (EXP1) and W_MDPI (EXP1) in a) USCRN forest and b) NEON forest sites.

In Fig. 8, we explored this error in SM estimation as a function of VOD (or NDVI) and MPDI. The green dots indicate the SM bias change that arises from the switch from SCA to EXP1, demonstrating the effect of incorporating NDVI τ-ω. The orange dots represent the change in SM bias from EXP1 to EXP2, displaying the influence of MPDI on the accuracy of SM. The majority of the unrealistic SM overestimations are rectified within the reasonable SM range. This improvement is evident from the increase in green data points after incorporating NDVI and MPDI parameters for τ and ω, as depicted in Figure 7a. While high VOD (> 0.6) benefits from the ω parameterization with NDVI, some overestimation issues persist across all VOD ranges. However, the MPDI parameterization has effectively mitigated this error by increasing ω and decreasing τ (or absorption), particularly when MPDI values are elevated, as shown in Figure 8c.

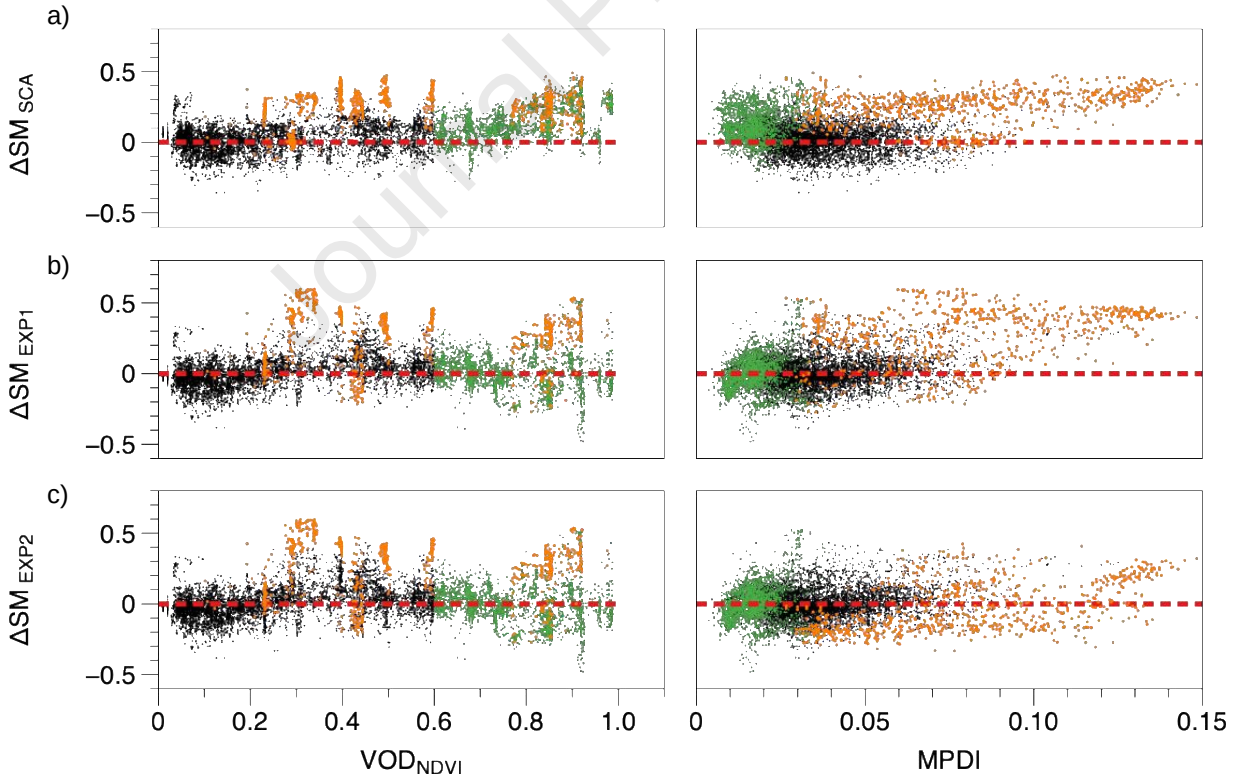

Fig. 8 SM estimation error along VOD (or NDVI) and MPDI (green dots: SM bias change from SCA to EXP1, showing the effect by the incorporation of the NDVI τ-ω, orange dots: the SM

bias change from EXP1 to EXP2, highlighting the impact of MPDI on SM accuracy) in USCRN; SM bias error by a) SCA method, b) EXP1 and c) EXP2.

Figure 9 illustrates an evident improvement. The high positive SM errors, represented by red dots in both SCA (ΔSM SCA) and the NDVI-based τ-ω model (ΔSM EXP1), have been effectively reduced, now falling within the moderate SM error range (less than 0.2 $cm^3\ cm^{-3}$), as highlighted by the green dots in Figure 9.

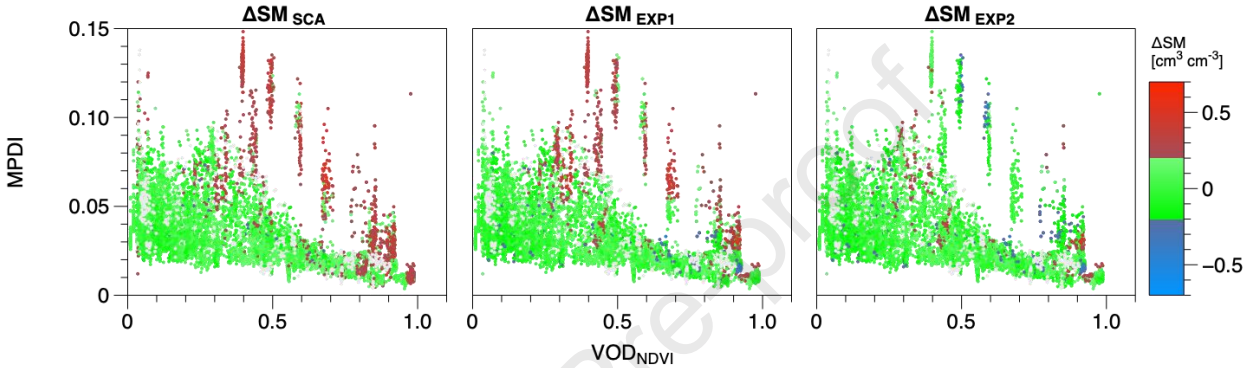

Fig. 9 The SM error distribution in NDVI x -axis and MPDI y-axis (green: acceptable, red: severely positive, blue: severely negative SM error)

5. Discussion

5.1 Mismatching issue

The comparisons of SMAP SM with in situ measurements can result in large errors because of the representativeness differences between satellite observations and in situ measurements (e.g., Gruber et al., 2020; Montzka et al., 2020; Colliander et al., 2022;). This study shows that SMAP SM is unrealistically high in dense vegetation regions, even without comparing to in situ data. This is due to the radiative transfer model (RTM) not considering dynamic scattering albedo varying with NDVI and MPDI. The proposed new τ-ω model reduced these positive bias errors related to VOD or MPDI.

5.2 NDVI issue

5.2.1 NDVI saturation in dense vegetation

Various studies demonstrated the MODIS-based VOD used in the SCA (τ_{NDVI}) can produce errors for SM estimation (Chaubell et al., 2020; Dong et al., 2018). For example, SM error can be

caused by the saturation of NDVI in dense vegetation. However, this is unlikely to cause SM overestimation. If the real VOD is higher than the saturated τ_{NDVI}, Tb will increase, exacerbating the overestimation of SM based on Fig.3.a.

One of the emerging method is a kernel NDVI (k-NDVI) (Camps-Valls, et al., 2021, Wang et al., 2023) to solve the NDVI saturation issue in the forested regions. However, this technique employs a kernel function sometimes masking the essential physical processes, complicating the understanding of its outcomes. Our research presents a solution rooted in physical principles, effectively addressing this limitation. We characterize the fluctuations of the τ and ω parameters as they relate not only to NDVI, but also MPDI. By fine-tuning the τ parameter associated with NDVI in combination with MPDI, we have directly tackled the issue of saturation in dense vegetation—a critical challenge for conventional NDVI-based VOD applications. This adjustment emerges as a vital strategy for overcoming the saturation hurdle, allowing for the extraction of pertinent vegetation parameters. Consequently, our methodology not only resolves the overestimation issue of soil moisutre in forest but also sheds light on the physical processes driving variations in vegetation signals, providing more understanding of these dynamics in forest. In a future study, we will pursue the synergy between more adavnced approaches, such as k-NDVI, and our physical based MPDI consideration for further improvements in the soil moisture estimation from microwave Tb over dense forest.

5.2.2 Climatological NDVI input in RTM

As shown in Fig. 10, the SM SCA (gray curve from -110 to -98) is systematically underestimated under crops and grass classified by IGBP in the top panel of the figure. One possible cause of this issue is the use of MODIS VOD in SCA, which is the monthly average over 10 years. In the real world, vegetation changes every year, especially cropland, due to different agricultural practices. The average VOD from MODIS applied in SCA decreases in the west as increasing VOD with longitude increase depicted in Fig.10. The gradual decrease of VOD in this region (longitude from -110 to -98) may be caused by averaging temporal patterns in each pixel, which is a definite discrepancy from the more temporally and spatially highly resolved snapshot measurements from VIIRS and lidar. The opposite case (lower τ, lower SM estimation) can also be seen, where the NDVI VOD (monthly averaged VOD) is higher than the VIIRS VOD (more real-time VOD), where the NDVI based SM showed underestimation due to lower NDVI τ than

real VIIRS τ as shown in Fig. 10. In other words, the replacement of NDVI VOD with VIIRS VOD can be a further improvement of the current τ-ω model.

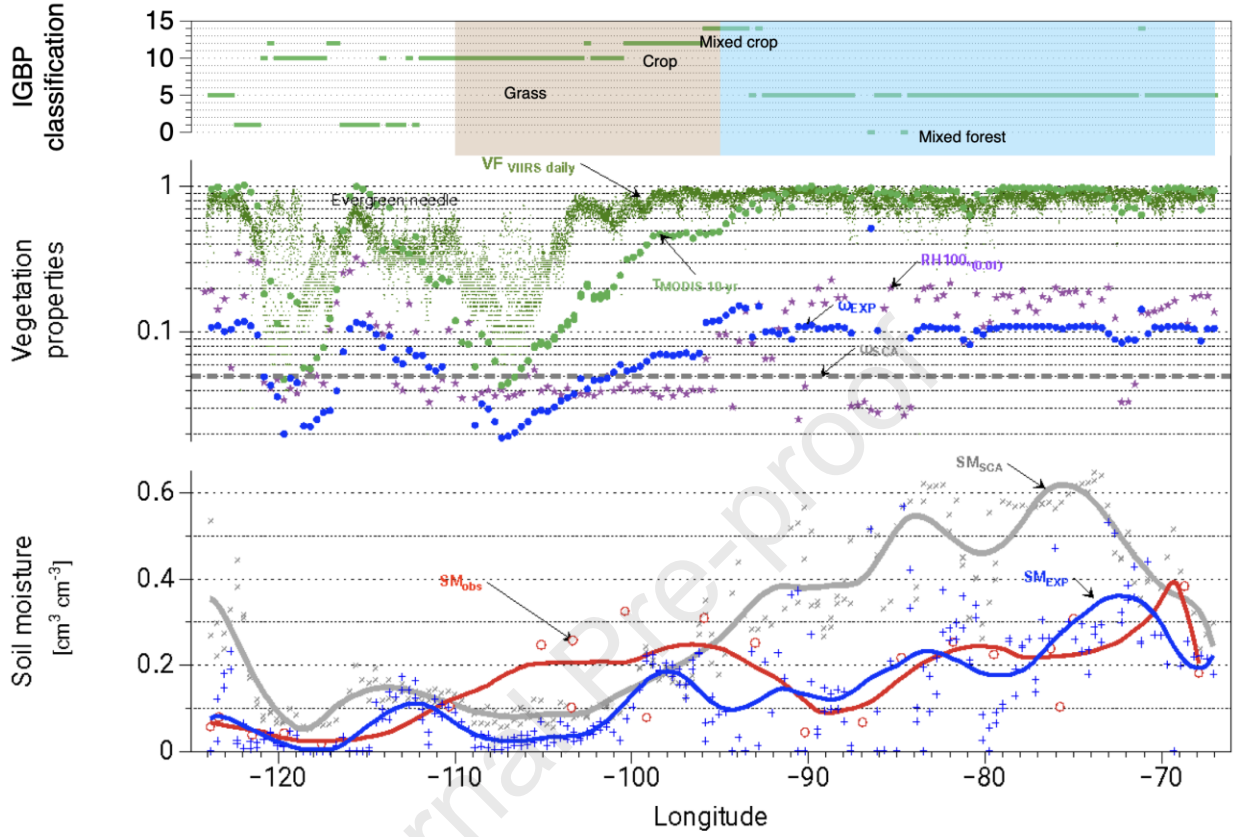

Fig. 10 Longitudinal comparisons of SCA and EXP (modified) soil moisture (smooth fit soil moisture curve for gray: SCA, for blue: proposed approach and red: *in situ* soil moisture measurements) with scattering albedo applied in SCA and EXP1 and other vegetation properties (vegetation fractions from VIIRS daily observation, MODIS 10 year daily average and NASA spaceborne lidar measurement GEDI (RH100 global forest canopy height in m) (scaled by dividing 100 in this study).

5.3 Absorption issue rather than scattering albedo

The recent study (Bauer et al., 2021) found that the scattering changes over time are not as significant as absorption in dense vegetation. In nature it is obvious that if the leaves just start growing or dying, not only VOD increases and decreases, but also the scattering albedo should change by leaves number and size (Park et al., 2020). Therefore, with higher NDVI both τ and ω should increase.

5.4 Issue by missing consideration of VWC effect

The seasonal increase in τ_{NDVI} (green dots in August in Fig.11) is also a valid indicator of changes in leaf size and number in forest, leading to an increase in scattering probability because τ_{NDVI} is positively propotional to NDVI based leaf area index (LAI). This consideration has been considered by the NDVI-based allometric approach (Park et al., 2020). However, the NDVI can be high in the summer because plants have a higher volumetric water content (VWC), absorbing more than they scatter, according to a study by Bauer et al. (2021). This adjustment (scattering decreases but absorption increases) has been done by adjustment with low MPDI input (purple dots in August in Fig. 11) according to Fig. 3c.

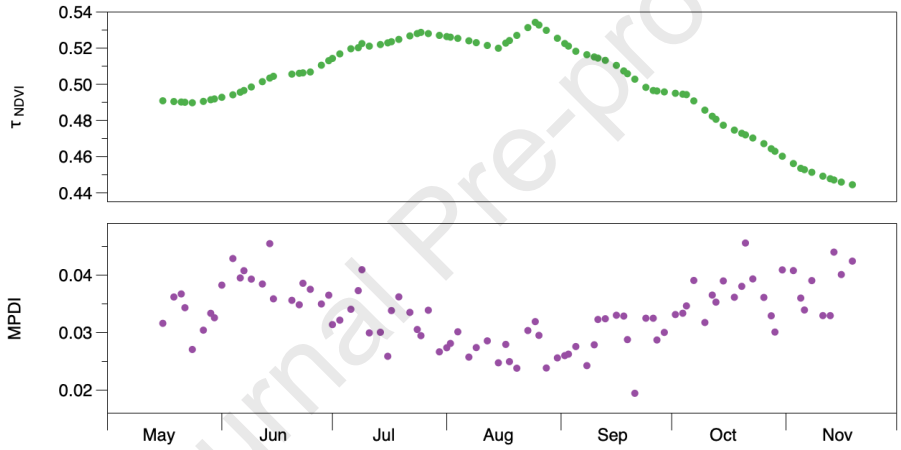

Fig. 11 The seasonal change of NDVI τ and MPDI in Avondale-2-N (USCRN; lat: 39.8593, lon: -75.7861)

5.5 Relationship between vegetation density and MPDI

The NDVI exhibits a positive correlation with vegetation density. However, the relationship between vegetation density and the MPDI tends to be inversely proportional, as indicated by the scatterplots of NDVI and MPDI in Fig. 2 and the dynamics of NDVI and MPDI in Fig. 11. Nevertheless, this relationship alone cannot always accurately determine vegetation density from MPDI. When vegetation primarily consists of horizontally oriented leaves, the MPDI can increase the scattering albedo in horizontally polarized waves, even in high vegetation density. As a result, the MPDI can increase independently from vegetation density or, for the same vegetation density, MPDI can vary for different vegetation types. Consequently, using only MPDI or NDVI alone

cannot effectively improve the τ-ω model in a realistic manner. To accurately reflect vegetation density and vegetation structure in the τ-ω model, it is necessary to incorporate both NDVI and MPDI, as shown in Fig .3.

5.6 Heterogeneity issue

SM is frequently overestimated by SCA. This problem has been partially addressed by using a dynamic scattering albedo that is parameterized with VOD (Park et al., 2020). However, SM is still overestimated in low Tb ranges (Tb < 230K) where they are classified as inhomogeneous vegetation, such as mixed forests and mixed crops, as Figure 12 shows. This can be attributed to the fact that the heterogeneity of the landscape leads to a clear distinction between TBv and TBh.

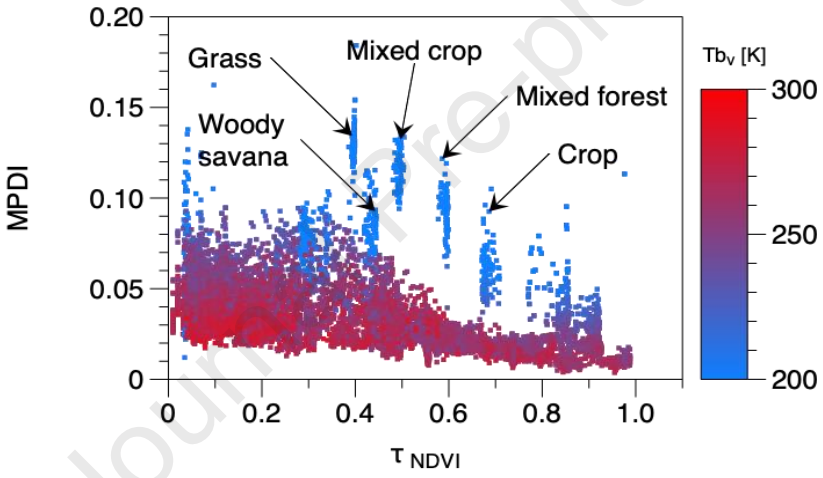

Fig. 12 SMAP soil moisture error in low Tb (<230K) with NDVI, MPDI and IGBP information

This study first presents the integration of NDVI (vegetation health state) and MPDI (vegetation structural state) into the existing τ-ω model showing the improvement in SM estimation with higher correlation and lower ubRMSE.

5.7 c_{IGBP} simplification issue

5.7.1 Missing height variability in c_{IGBP}

Based on the inverse relationship between c_{IGBP} and h shown in Eq. (3), the high average h for forests compared to grasslands or crops should lead to a lower value of c_{IGBP}. As shown in Table 2, the c_{IGBP} values of forests found with the least error tend to be lower than those of crops and

grasses. Although c_{IGBP} is a complex number that is determined by four parameters (b, ρ_E, c, and h), this study assumed that all these parameters are mainly determined by vegetation type according to the IGBP classification, rather than identifying each component. This approach is practical, but it still contains some uncertainty due to its physical simplification. In a future study, further improvement can be expected by specifying those parameters in each SMAP grid.

5.7.2 Missing b parameter variability in c_{IGBP}

Similar to the mixed forest, the mixed crop sites suffer the issue in the SM estimated by the proposed τ-ω model. For example, by the plant classification by C3 or C4, the b parameter, compounded in c_{IGBP} in our study, has been specified in more detail in various studies (e.g., Jackson, 1993; Jackson & Schmugge, 1991; Saleh et al., 2007; Wigneron et al., 2003). A further differentiation of c_{IGBP} similar to existing global information of b parameter provided by SMAPL3 products might be a possible option to tackle this issue. Another way to solve this challenge is to apply various studies about the allometry of vegetation (Asner et al., 2013; Asner & Mascaro, 2014; Chambers et al., 2001; Chave et al., 2005, 2014). These studies are helpful to consider a more specific ratio between height and area for different types of crops within the allometry parameters. This kind of further sub-classification within the IGBP cropland classification is necessary.

Another potential reason is the spatial heterogeneity assumption within one SMAP grid granule. If a SMAP granule, classified as cropland, contains several mixed surface types, for example 34% cropland, 33% forest and 33% grass, one single allometry parameter (used for cropland) might cause a large uncertainty for the τ-ω unified model. Hence, in the next research study, it is necessary to focus on the classification issue (for example C3/C4) as well as on the heterogeneity issue and how these problems can be solved.

5.8 Roughness model issue

The error of SMAP SCA is also highly affected by the uncertainty of the soil roughness parameters. However, if the SM estimated by SCA becomes uncertain due to the roughness model, it should explain why this error happens especially in dense vegetation and should demonstrate this can be really the solution to relate to the SM overestimation issue of SCA. Arguably, soil roughness in more vegetated regions will be higher than less vegetated or bare soil. In forest, due

to the litter falls and surface-emerging root system, the soil tends to be rougher than for non or less vegetated areas (Shroder, 2013). Furthermore, because of the litter, moss, and other top-of-surface layers, the air-soil interface is not cleanly defined, affecting the roughness parameterization and likely increasing the effective value of h. Therefore, the real soil roughness is likely higher than assumed in SCA. In this case, the RTM simulation of microwave Tb will be higher. However, this consideration will exacerbate the SM overestimation rather than mitigating because of the necessity of wetter soil conditions to simulate Tb close to the measured Tb. The SM overestimation does not originate from the unrealistic roughness parameter model and the improvement of the roughness model cannot be a solution for the SCA issue presented in this study. Therefore, this study applied the same roughness parameters used in the SCA approach to demonstrate the improvement by the proposed τ-ω model.

5.9 Dielectric mixing model issue

Another way to improve the SM retrieval accuracy is within the soil part looking into the dielectric mixing model. The dielectric mixing model shown in Fig. 2 is important for the accurate estimation of SM from microwave Tb because it simulates the effective dielectric constant of wet soil (mixture of minerals and water). One of the main uncertainties in this simulation is the ratio of free to bound water in the soil. Because bound water has a much lower dielectric constant compared to free water (80), a dielectric mixing model not considering the bound water increase due to the soil organic matter will underestimate the microwave Tb (Park et al., 2017). To simulate microwave Tb more accurately in this study, a more recent dielectric mixing model was applied, considering organic matter (Park et al., 2019; Park et al., 2021). Currently, the dielectric mixing model is the function of soil organic carbon such as wilting point, saturation point, and the bound water dielectric constant and the dielectric constant of dried organic carbon. This model is validated by comparison with *in situ* SM and *in situ* soil organic carbon. Then, this model was applied with input of a soil organic matter map (from SoilGrid250m, Hengl et al., 2014, 2017). This map can have errors for some land use or regions in the world. In the future, this needs to be investigated as well.

5.10 MPDI ambiguity

MPDI is not solely influenced by vegetation but can also be influenced by other environmental factors like soil roughness, moisture (Chen et al., 2018), or snow. Therefore, relying solely on the

τ-ω model with MPDI can introduce uncertainty when the vegetation effect is minimal compared to soil effects. To address this, it is first crucial to precisely discern whether the measured MPDI was determined by the emission signal of the contributions of soil and vegetation. The strong correlation of SM with MPDI presented in Chen et al., 2018 could have been originated from the strong correlation between vegetation and SM, in which case the MPDI is correlated with the polarizing effects of the vegetation rather than those of SM. After this investigation, soil and vegetation contributions can be incorporated into the dielectric mixing model and roughness model. While in-depth ground surveys and frequency-specific analyses could potentially resolve this ambiguity, such approaches are beyond the scope of our current research. However, it is important to note that in dense forests, MPDI significantly reduces uncertainty, as demonstrated in our study.

5.11 Application to DCA

In a future study, the application to the current DCA will be pursued. In the DCA approach, NDVI input is not necessary. Therefore, to apply the method to the current DCA, the TB will be simulated close to the observed SMAP Tb with the optimal VOD (not calculated with NDVI) searched with ω changed by the VOD and the additional input of MPDI.

5.12 Application to level 4 product

The observation operator with the improved τ-ω can be used with better accuracy for data assimilation products such as SMAPL4. The improvement in the accuracy of SMAPL4 owing to the new τ-ω model with MPDI input might be interesting to see. When such satellite soil moisture is used for model validation (Yuan & Quiring, 2017) such as CMIP5, the performance of the model is evaluated incorrectly, and when used for data assimilation of the estimated soil moisture rather than brightness temperature from satellite (Nambiar et al., 2020), the improvement effect of model prediction by initialization on soil moisture cannot be anticipated. Furthermore, soil moisture extremes present during, or preceding climate extremes associated with droughts and floods cannot be adequately detected over these regions.

6. Summary

Even microwaves with long wavelengths capability cannot accurately estimate soil moisture (SM) from satellites over some agricultural and forested areas due to dense vegetation (Yarri et al. 2019). But this study started with the hypothesis that the limitation of SM estimation from dense vegetation is not the thick optical opacity of the vegetation, but the vegetation scattering albedo improperly considered in the RTM severely affected especially in dense vegetation. In this study, the SM estimation (Park et al., 2020) is more accurate than the constant ω approach (SCA and DCA) but still overestimated regardless of applying the NDVI-based varying ω in the SM retrieval. The hypothesis is that the missing polarization information for vegetation structural property is the main uncertainty in the NDVI-based-supported, time-dynamic τ-ω model. The method presented here derives a fraction factor from the microwave polarization difference index (MPDI) to adjust the NDVI-based τ and ω. The results show that the modified retrieval provides more accurate estimates of SM.

In most of the studies, the SM products from dense forest areas have been excluded in most of the validation studies (Fan et al., 2020; Li et al., 2022; Ma et al., 2023). However, based on the proposed microwave RTMs, extreme hydrological events such as floods and droughts in densely vegetated areas can be adequately detected or monitored. Furthermore, owing to the proposed approach, various studies using SMAP SM products as well as vegetation optical depth over dense vegetation areas (Chaparro et al., 2022; Zwieback et al., 2019), downscaling (Das et al., 2018; Mishra et al., 2018), machine learning (Lee et al., 2022) and SM monitoring study (Mladenova et al., 2019) will be able to be more extensively performed.

Acknowledgement

This work was funded by the Korea Meteorological Administration Research and Development Program “Development of Climate Prediction System” under Grant (KMA2018-00322). The USDA is an equal opportunity employer and provider. A contribution to this work was made at the Jet Propulsion Laboratory, California Institute of Technology, under a contract with National Aeronautics and Space Administration and a National Research Foundation of Korea Grant from the Korean Government (MSIT) (RS-2022-00165656).

References

Al-Yaari, A., Wigneron, J. P., Dorigo, W., Colliander, A., Pellarin, T., Hahn, S., Mialon, A., Richaume, P., Fernandez-Moran, R., Fan, L., Kerr, Y. H., & de Lannoy, G. (2019). Assessment and inter-comparison of recently developed/reprocessed microwave satellite soil moisture products using ISMN ground-based measurements. *Remote Sensing of Environment, 224*. https://doi.org/10.1016/j.rse.2019.02.008

Ambadan, J. T., MacRae, H. C., Colliander, A., Tetlock, E., Helgason, W., Gedalof, Z. E., & Berg, A. A. (2022). Evaluation of SMAP Soil Moisture Retrieval Accuracy Over a Boreal Forest Region. *IEEE Transactions on Geoscience and Remote Sensing*, *18*.

Asner, G. P., & Mascaro, J. (2014). Mapping tropical forest carbon: Calibrating plot estimates to a simple LiDAR metric. *Remote Sensing of Environment*, *140*, 614–624. https://doi.org/10.1016/j.rse.2013.09.023

Asner, G. P., Mascaro, J., Anderson, C., Knapp, D. E., Martin, R. E., Kennedy-Bowdoin, T., van Breugel, M., Davies, S., Hall, J. S., Muller-Landau, H. C., Potvin, C., Sousa, W., Wright, J., & Bermingham, E. (2013). High-fidelity national carbon mapping for resource management and REDD+. *Carbon Balance and Management*, *8*(1), 1–14. https://doi.org/10.1186/1750-0680-8-7

Ayres, E., Colliander, A., Cosh, M. H., Roberti, J. A., Simkin, S., & Genazzio, M. A. (2021). Validation of SMAP Soil Moisture at Terrestrial National Ecological Observatory Network (NEON) Sites Show Potential for Soil Moisture Retrieval in Forested Areas. *IEEE Journal of Selected Topics in Applied Earth Observations and Remote Sensing*, *14*. https://doi.org/10.1109/JSTARS.2021.3121206

Baur, M. J., Jagdhuber, T., Feldman, A. F., Chaparro, D., Piles, M., & Entekhabi, D. (2021). Time-variations of zeroth-order vegetation absorption and scattering at L-band. Remote Sensing of Environment, 267, 112726.

Becker, F., & Choudhury, B. J. (1988). Relative sensitivity of normalized difference vegetation index (NDVI) and microwave polarization difference index (MPDI) for vegetation and desertification monitoring. Remote sensing of environment, 24(2), 297-311.

Bircher, S., Andreasen, M., Vuollet, J., Vehviläinen, J., Rautiainen, K., Jonard, F., Weihermüller, L., Zakharova, E., Wigneron, J. P., & H Kerr, Y. (2016). Soil moisture sensor calibration for organic soil surface layers. *Geoscientific Instrumentation, Methods and Data Systems*, *5*(1). https://doi.org/10.5194/gi-5-109-2016

Camps-Valls, G., Campos-Taberner, M., Moreno-Martínez, Á., Walther, S., Duveiller, G., Cescatti, A., ... & Running, S. W. (2021). A unified vegetation index for quantifying the terrestrial biosphere. *Science Advances*, *7*(9), eabc7447.

Chambers, J. Q., Santos, J. dos, Ribeiro, R. J., & Higuchi, N. (2001). Tree damage, allometric relationships, and above-ground net primary production in central Amazon forest. *Forest Ecology and Management*, *152*(1–3), 73–84. https://doi.org/10.1016/S0378-1127(00)00591-0

Chaparro, D., Feldman, A. F., Chaubell, M. J., Yueh, S. H., & Entekhabi, D. (2022). Robustness of Vegetation Optical Depth Retrievals Based on L-Band Global Radiometry. *IEEE Transactions on Geoscience and Remote Sensing*, *60*, 1–17. https://doi.org/10.1109/TGRS.2022.3201581

Chave, J., Andalo, C., Brown, S., Cairns, M. A., Chambers, J. Q., Eamus, D., Fölster, H., Fromard, F., Higuchi, N., Kira, T., Lescure, J. P., Nelson, B. W., Ogawa, H., Puig, H., Riéra, B., & Yamakura, T. (2005). Tree allometry and improved estimation of carbon stocks and balance in tropical forests. *Oecologia*, *145*(1), 87–99. https://doi.org/10.1007/s00442-005-0100-x

Chave, J., Réjou-Méchain, M., Búrquez, A., Chidumayo, E., Colgan, M. S., Delitti, W. B. C., Duque, A., Eid, T., Fearnside, P. M., Goodman, R. C., Henry, M., Martínez-Yrízar, A., Mugasha, W. A., Muller-Landau, H. C., Mencuccini, M., Nelson, B. W., Ngomanda, A., Nogueira, E. M.,

Ortiz-Malavassi, E., … Vieilledent, G. (2014). Improved allometric models to estimate the aboveground biomass of tropical trees. *Global Change Biology*, *20*(10), 3177–3190. https://doi.org/10.1111/gcb.12629

Chen, Q., Zeng, J., Cui, C., Li, Z., Chen, K. S., Bai, X., & Xu, J. (2017). Soil moisture retrieval from SMAP: a validation and error analysis study using ground-based observations over the little Washita watershed. *IEEE Transactions on Geoscience and Remote Sensing*, *56*(3), 1394-1408.

Colliander, A., Cosh, M. H., Kelly, V. R., Kraatz, S., Bourgeau-Chavez, L., Siqueira, P., Roy, A., Konings, A. G., Holtzman, N., Misra, S., Entekhabi, D., O'Neill, P., & Yueh, S. H. (2020). SMAP Detects Soil Moisture Under Temperate Forest Canopies. *Geophysical Research Letters*, *47*(19). https://doi.org/10.1029/2020GL089697

Colliander, A., Jackson, T. J., Berg, A., Bosch, D. D., Caldwell, T., Chan, S., Cosh, M. H., Collins, C. H., Martínez-Fernández, J., McNairn, H., Prueger, J. H., Starks, P. J., Walker, J. P., & Yueh, S. H. (2020). Effect of Rainfall Events on SMAP Radiometer-Based Soil Moisture Accuracy Using Core Validation Sites. In Journal of Hydrometeorology (Vol. 21, Issue 2, pp. 255–264). American Meteorological Society. https://doi.org/10.1175/jhm-d-19-0122.1

Colliander, A., Reichle, R. H., Crow, W. T., Cosh, M. H., Chen, F., Chan, S., Das, N. N., Bindlish, R., Chaubell, J., Kim, S., Liu, Q., O'Neill, P. E., Dunbar, R. S., Dang, L. B., Kimball, J. S., Jackson, T. J., Al-Jassar, H. K., Asanuma, J., Bhattacharya, B. K., … Yueh, S. H. (2022). Validation of Soil Moisture Data Products From the NASA SMAP Mission. IEEE Journal of Selected Topics in Applied Earth Observations and Remote Sensing (Vol. 15, pp. 364–392). https://doi.org/10.1109/jstars.2021.3124743

Das, N. N., Entekhabi, D., Dunbar, R. S., Colliander, A., Chen, F., Crow, W., Jackson, T. J., Berg, A., Bosch, D. D., Caldwell, T., Cosh, M. H., Collins, C. H., Lopez-Baeza, E., Moghaddam, M., Rowlandson, T., Starks, P. J., Thibeault, M., Walker, J. P., Wu, X., … Njoku, E. G. (2018). The SMAP mission combined active-passive soil moisture product at 9 km and 3 km spatial resolutions. *Remote Sensing of Environment*, *211*, 204–217. https://doi.org/10.1016/j.rse.2018.04.011

Diamond, H. J., Karl, T. R., Palecki, M. A., Baker, C. B., Bell, J. E., Leeper, R. D., Easterling, D. R., Lawrimore, J. H., Meyers, T. P., Helfert, M. R., Goodge, G., & Thorne, P. W. (2013). U.S. Climate Reference Network after One Decade of Operations: Status and Assessment. *Bulletin of the American Meteorological Society*, *94*(4), 485-498. https://doi.org/10.1175/BAMS-D-12-00170.1

Dong, J., Crow, W. T., & Bindlish, R. (2018). The error structure of the SMAP single and dual channel soil moisture retrievals. Geophysical research letters, 45(2), 758-765.

Entekhabi, D., Reichle, R.H., Koster, R.D., Crow, W.T., 2010. Performance metrics for soil moisture retrievals and application requirements. J. Hydrol. 11, 832-840.

Fan, X., Liu, Y., Gan, G., & Wu, G. (2020). SMAP underestimates soil moisture in vegetation-disturbed areas primarily as a result of biased surface temperature data. *Remote Sensing of Environment*, *247*. https://doi.org/10.1016/j.rse.2020.111914

Feldman, A. F., Akbar, R., & Entekhabi, D. (2018). Characterization of higher-order scattering from vegetation with SMAP measurements. *Remote Sensing of Environment*, *219*, 324–338. https://doi.org/10.1016/j.rse.2018.10.022

Fernandez-Moran, R., Wigneron, J. P., Lopez-Baeza, E., Al-Yaari, A., Coll-Pajaron, A., Mialon, A., Miernecki, M., Parrens, M., Salgado-Hernanz, P. M., Schwank, M., Wang, S., & Kerr, Y. H. (2015). Roughness and vegetation parameterizations at L-band for soil moisture retrievals over

a vineyard field. *Remote Sensing of Environment*, *170*, 269–279. https://doi.org/10.1016/j.rse.2015.09.006

Fernandez-Moran, R., Wigneron, J., Lannoy, G., López-Baeza, E., Parrens, M., Mialon, A., Mahmoodi, A., Al-Yaari, A., Bircher, S., Bitar, A., Richaume, P., & Kerr, Y. (2017). A new calibration of the effective scattering albedo and soil roughness parameters in the SMOS SM retrieval algorithm. *Int. J. Appl. Earth Obs. Geoinformation*, 62, 27-38. https://doi.org/10.1016/j.jag.2017.05.013.

Gruber, Alexander, Lannoy, De, Gabrielle, Albergel, Clement, Al-Yaari, Amen, Luca, Brocca, Calvet, Colliander, Andreas, Cosh, Michael, Crow, Wade, Dorigo, Wouter, 2020. Validation practices for satellite soil moisture retrievals: what are (the) errors? Remote Sens. Environ. 244, 111806.

Hengl, T., de Jesus, J. M., MacMillan, R. A., Batjes, N. H., Heuvelink, G. B. M., Ribeiro, E., Samuel-Rosa, A., Kempen, B., Leenaars, J. G. B., Walsh, M. G., and Gonzalez, M. R.: SoilGrids1km – Global Soil Information Based on Automated Mapping, PLOS ONE, 9, e105992, https://doi.org/10.1371/journal.pone.0105992, 2014.

Hengl, T., de Jesus, J. M., Heuvelink, G. B. M., Gonzalez, M. R., Kilibarda, M., Blagoti´c, A., Shangguan, W., Wright, M. N., Geng, X., Bauer-Marschallinger, B., Guevara, M. A., Vargas, R., MacMillan, R. A., Batjes, N. H., Leenaars, J. G. B., Ribeiro, E., Wheeler, I., Mantel, S., and Kempen, B.: SoilGrids250m: Global gridded soil information based on machine learning, PLOS ONE, 12, e0169748, https://doi.org/10.1371/journal.pone.0169748, 2017.

Jackson, T. J. (1993). III. Measuring surface soil moisture using passive microwave remote sensing. *Hydrological Processes*, *7*(2). https://doi.org/10.1002/hyp.3360070205

Jackson, T. J., & Schmugge, T. J. (1991). Vegetation effects on the microwave emission of soils. *Remote Sensing of Environment*, *36*(3), 203–212. https://doi.org/10.1016/0034-4257(91)90057-D

Jeu, R. A. M., Wagner, W., Holmes, T. R. H., Dolman, A. J., Giesen, N. C., & Friesen, J. (2008). Global soil moisture patterns observed by space borne microwave radiometers and scatterometers. *Surveys in Geophysics*, *29*(4–5). https://doi.org/10.1007/s10712-008-9044-0

Konings, A. G., Piles, M., Das, N., & Entekhabi, D. (2017). L-band vegetation optical depth and effective scattering albedo estimation from SMAP. *Remote Sensing of Environment*, *198*, 460–470. https://doi.org/10.1016/j.rse.2017.06.037

Konings, A. G., Piles, M., Rötzer, K., McColl, K. A., Chan, S. K., & Entekhabi, D. (2016). Vegetation optical depth and scattering albedo retrieval using time series of dual-polarized L-band radiometer observations. *Remote Sensing of Environment*, *172*, 178–189. https://doi.org/10.1016/j.rse.2015.11.009

Kurum, M. (2013). Quantifying scattering albedo in microwave emission of vegetated terrain. Remote Sensing of Environment, 129, 66-74.

Lee, J., Park, S., Im, J., Yoo, C., & Seo, E. (2022). Improved soil moisture estimation: Synergistic use of satellite observations and land surface models over CONUS based on machine learning. *Journal of Hydrology*, *609*. https://doi.org/10.1016/j.jhydrol.2022.127749

Li, X., Wigneron, J.-P., Fan, L., Frappart, F., Yueh, S. H., Colliander, A., Ebtehaj, A., Gao, L., Fernandez-Moran, R., Liu, X., Wang, M., Ma, H., Moisy, C., & Ciais, P. (2022). A new SMAP soil moisture and vegetation optical depth product (SMAP-IB): Algorithm, assessment and inter-comparison. *Remote Sensing of Environment*, *271*, 112921. https://doi.org/https://doi.org/10.1016/j.rse.2022.112921

Ma, H., Li, X., Zeng, J., Zhang, X., Dong, J., Chen, N., Fan, L., Sadeghi, M., Frappart, F., Liu, X., Wang, M., Wang, H., Fu, Z., Xing, Z., Ciais, P., & Wigneron, J.-P. (2023). An assessment of L-band surface soil moisture products from SMOS and SMAP in the tropical areas. *Remote Sensing of Environment*, *284*, 113344. https://doi.org/https://doi.org/10.1016/j.rse.2022.113344

Mironov, V. L., Kosolapova, L. G., Fomin, S. v., & Savin, I. v. (2019). Experimental analysis and empirical model of the complex permittivity of five organic soils at 1.4 GHz in the Temperature Range from -30 °c to 25 °c. *IEEE Transactions on Geoscience and Remote Sensing*, *57*(6), 3778–3787. https://doi.org/10.1109/TGRS.2018.2887117

Mironov, V. L., Kosolapova, L. G., Fomin, S. v., Savin, I. v., & Muzalevskiy, K. v. (2018). Dielectric model for thawed and frozen organic soils at 1.4 GHz. *International Geoscience and Remote Sensing Symposium (IGARSS)*, *2018-July*, 7180–7183. https://doi.org/10.1109/IGARSS.2018.8518443

Mishra, V., Ellenburg, W. L., Griffin, R. E., Mecikalski, J. R., Cruise, J. F., Hain, C. R., & Anderson, M. C. (2018). An initial assessment of a SMAP soil moisture disaggregation scheme using TIR surface evaporation data over the continental United States. *International Journal of Applied Earth Observation and Geoinformation*, *68*. https://doi.org/10.1016/j.jag.2018.02.005

Mladenova, I. E., Bolten, J. D., Crow, W. T., Sazib, N., Cosh, M. H., Tucker, C. J., & Reynolds, C. (2019). Evaluating the Operational Application of SMAP for Global Agricultural Drought Monitoring. *IEEE Journal of Selected Topics in Applied Earth Observations and Remote Sensing*, *12*(9). https://doi.org/10.1109/JSTARS.2019.2923555

Montzka, C., M. Cosh, B. Bayat, A. Al Bitar, A. Berg, R. Bindlish, H. R. Bogena, J. D. Bolten, F. Cabot, T. Caldwell, S. Chan, A. Colliander, W. Crow, N. Das, G. De Lannoy, W. Dorigo, S. R. Evett, A. Gruber, S. Hahn, T. Jagdhuber, S. Jones, Y. Kerr, S. Kim, C. Koyama, M. Kurum, E. Lopez-Baeza, F. Mattia, K. McColl, S. Mecklenburg, B. Mohanty, P. O Ì• Neill, D. Or, T. Pellarin, G. P. Petropoulos, M. Piles, R. H. Reichle, N. Rodriguez-Fernandez, C. Rüdiger, T. Scanlon, R. C. Schwartz, D. Spengler, P. Srivastava, S. Suman, R. van der Schalie, W. Wagner, U. Wegmüller, J.-P. Wigneron, F. Camacho, and J. Nickeson (2020): Soil Moisture Product Validation Good Practices Protocol Version 1.0. In: C. Montzka, M. Cosh, J. Nickeson, F. Camacho (Eds.): *Good Practices for Satellite-Derived Land Product Validation* (p. 123), Land Product Validation Subgroup (WGCV/CEOS), doi:10.5067/doc/ceoswgcv/lpv/sm.001

Nambiar, M. K., Ambadan, J. T., Rowlandson, T., Bartlett, P., Tetlock, E., & Berg, A. A. (2020). Comparing the assimilation of SMOS brightness temperatures and soil moisture products on hydrological simulation in the canadian land surface scheme. *Remote Sensing*, *12*(20). https://doi.org/10.3390/rs12203405

O'Neill, E. Njoku, T. Jackson, S. Chan, R. Bindlish, J. Chaubell. SMAP algorithm theoretical basis document: level 2 & 3 soil moisture (passive) data products, Revision F, Jet Propulsion Lab., California Inst. Technol., Pasadena, CA, USA (2020). (JPL D-66480)

O'Neill, P., Bindlish, R., Chan, S., Njoku, E., & Jackson, T. Algorithm theoretical basis document. Level 2 & 3 soil moisture (passive) data products, Jet Propulsion Lab., California Inst. Technol., Pasadena, CA, USA (2021)

Park, C. H., Berg, A., Cosh, M. H., Colliander, A., Behrendt, A., Manns, H., Hong, J., Lee, J., Zhang, R., & Wulfmeyer, V. (2021). An inverse dielectric mixing model at 50gMHz that considers soil organic carbon. *Hydrology and Earth System Sciences*, *25*(12). https://doi.org/10.5194/hess-25-6407-2021

Park, C., Montzka, C., Jagdhuber, T., Jonard, F., de Lannoy, G., Hong, J., Jackson, T. J., & Wulfmeyer, V. (2019). A Dielectric Mixing Model Accounting for Soil Organic Matter. *Vadose Zone Journal*, *18*(1), 190036. https://doi.org/10.2136/vzj2019.04.0036

Park, C.-H., Behrendt, A., LeDrew, E., & Wulfmeyer, V. (2017). New Approach for Calculating the Effective Dielectric Constant of the Moist Soil for Microwaves. *Remote Sensing*, *9*(7), 732. https://doi.org/10.3390/rs9070732

Park, C.-H., Jagdhuber, T., Colliander, A., Lee, J., Berg, A., Cosh, M., Kim, S.-B., Kim, Y., & Wulfmeyer, V. (2020). Parameterization of Vegetation Scattering Albedo in the Tau-Omega Model for Soil Moisture Retrieval on Croplands. *Remote Sensing*, *12*(18), 2939. https://doi.org/10.3390/rs12182939

Parrens, M., Wigneron, J., Richaume, P., Mialon, A., Bitar, A., Fernandez-Moran, R., Al-Yaari, A., & Kerr, Y. (2016). Global-scale surface roughness effects at L-band as estimated from SMOS observations.. *Remote Sensing of Environment*, 181, 122-136. https://doi.org/10.1016/J.RSE.2016.04.006.

Peng, B., Zhao, T., Shi, J., Lu, H., Mialon, A., Kerr, Y., Liang, X., & Guan, K. (2017). Reappraisal of the roughness effect parameterization schemes for L-band radiometry over bare soil. *Remote Sensing of Environment*, 199, 63-77. https://doi.org/10.1016/J.RSE.2017.07.006.

Saleh, K., Wigneron, J. P., Waldteufel, P., de Rosnay, P., Schwank, M., Calvet, J. C., & Kerr, Y. H. (2007). Estimates of surface soil moisture under grass covers using L-band radiometry. *Remote Sensing of Environment*, *109*(1), 42–53. https://doi.org/10.1016/j.rse.2006.12.002

Shroder, J. F. (2013). *Treatise on geomorphology* (Vol. 1). Academic Press.

Wang, Q., Moreno-Martínez, Á., Muñoz-Marí, J., Campos-Taberner, M., & Camps-Valls, G. (2023). Estimation of vegetation traits with kernel NDVI. *ISPRS Journal of Photogrammetry and Remote Sensing*, *195*, 408-417.

Wigneron, J. P., Calvet, J. C., Pellarin, T., van de Griend, A. A., Berger, M., & Ferrazzoli, P. (2003). Retrieving near-surface soil moisture from microwave radiometric observations: Current status and future plans. In *Remote Sensing of Environment* (Vol. 85, Issue 4, pp. 489–506). Elsevier Inc. https://doi.org/10.1016/S0034-4257(03)00051-8

Wigneron, J. P., Pardé, M., Waldteufel, P., Chanzy, A., Kerr, Y., Schmidl, S., & Skou, N. (2004). Characterizing the dependence of vegetation model parameters on crop structure, incidence angle, and polarization at L-band. IEEE Transactions on Geoscience and Remote Sensing, 42(2), 416-425.

Yuan, S., & Quiring, S. M. (2017). Evaluation of soil moisture in CMIP5 simulations over the contiguous United States using in situ and satellite observations. *Hydrology and Earth System Sciences*, *21*(4), 2203–2218. https://doi.org/10.5194/hess-21-2203-2017

Zhang, R., Kim, S., & Sharma, A. (2019). A comprehensive validation of the SMAP Enhanced Level-3 Soil Moisture product using ground measurements over varied climates and landscapes. *Remote Sensing of Environment*, *223*. https://doi.org/10.1016/j.rse.2019.01.015

Zwieback, S., Bosch, D. D., Cosh, M. H., Starks, P. J., & Berg, A. (2019). Vegetation–soil moisture coupling metrics from dual-polarization microwave radiometry using regularization. *Remote Sensing of Environment, 231*. https://doi.org/10.1016/j.rse.2019.111257

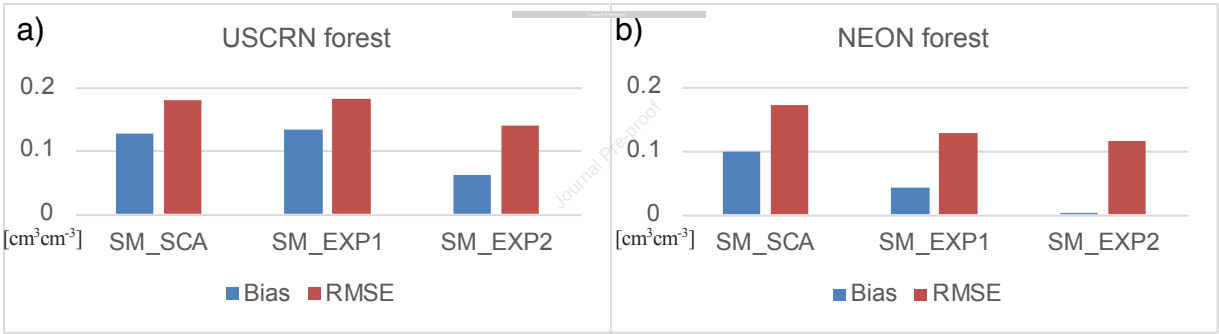

Highlights (for review)

- Optical depth increases with high NDVI and low MPDI.
- Scattering albedo increases with high NDVI and high MPDI.
- Increasing scattering albedo decreases brightness temperature in forward simulation.
- Decreased brightness temperature in simulation resolved overestimation of SMAP SM.
- L-band (1.4 GHz) radiometer measurements can assess forest soil moisture (SM).

Declaration of interests

☐ The authors declare that they have no known competing financial interests or personal relationships that could have appeared to influence the work reported in this paper.

☒ The authors declare the following financial interests/personal relationships which may be considered as potential competing interests:

Chang-Hwan Park reports financial support was provided by National Research Foundation of Korea Grant. Johan Lee reports financial support was provided by Korea Meteorological Administration. Kyung-On Boo reports financial support was provided by Korea Meteorological Administration.